Int. J. Heat Mass Transfer. Vol. 32, No. 5, pp. 881–888, 1989
Printed in Great Britain

0017–9310/89 $3.00+0.00
Pergamon Press plc

Mixed convection flow in a saturated porous annulus

K. MURALIDHAR
Department of Mechanical Engineering, Indian Institute of Technology, Kanpur 208016, India

(*Received* 29 *December* 1987 *and in final form* 4 *August* 1988)

Abstract—Mixed convective flow and heat transfer are considered in the annular region between concentric cylinders filled with fluid-saturated porous material. The inner cylinder is heated and the outer cylinder cooled. The heat transfer rate from the inner cylinder as a function of the superimposed flow is studied, allowing for possible buoyancy effects. Both horizontal and vertical annuli are included in the study. The equations governing flow are numerically solved. Results have been obtained for a range of Peclet numbers, $0 < Pe < 10$, and Rayleigh numbers, $0 < Ra < 500$. The mixed convection regime is expected to be predominant for this range of parameters.

INTRODUCTION

THE STUDY of flow and heat transfer in the annular region between concentric cylinders has applications in nuclear waste disposal research. It is proposed that cannisters filled with radioactive waste be buried in earth, so as to isolate them from the human population. It is of interest to know the surface temperature of these cannisters. This value would strongly depend on buoyancy-driven flow sustained by the heated surface, and the possible movement of ground water past it. This is the motivation behind studying mixed convection in a fluid-saturated porous medium contained in a cylindrical annulus.

Free convection in a vertical porous annulus has been extensively studied by Prasad [1], Prasad and Kulacki [2] and Prasad *et al.* [3], both theoretically and experimentally. Caltagirone [4] has published a detailed theoretical study of free convection in a horizontal porous annulus, including possible three-dimensional and transient effects. Similar studies for fluid-filled annuli are available in the literature, but will not be reviewed here (see, for example Rao *et al.* [5]). The forced convection problem has an analytical solution, which has been included in this paper. The mixed convection problem, however, appears unsolved for the annular configuration. Ranganathan and Viskanta [6] have studied mixed convection in the boundary-layer formed on a vertical flat plate bounding a porous medium. Much of the work referred to above pertains to a two-dimensional geometry, which in comparison to three dimensions provides an important simplification for computation. Mixed convection in a horizontal annulus leads to a fully three-dimensional flow field. In the present work, this is dealt with by parabolizing the set of governing equations.

FORMULATION

Steady flow in vertical and horizontal annuli is studied here. Flow in a porous medium is taken to be governed by Darcy's law [7]. Buoyancy is included through the Boussinesq approximation. The equations governing flow in a vertical annulus are two-dimensional, since the flow remains axisymmetric. This may be destroyed in long fluid-filled annuli, but this destruction of symmetry and formation of a roll pattern is related to the inertial terms of the Navier–Stokes equations. The assumption of two-dimensionality of Darcian flow, which does not have these inertial terms, is hence reasonable. For a horizontal annulus, the flow is essentially three-dimensional, with a primary flow parallel to its axis and buoyant flow providing a swirl to it.

Let (u, v, w) be components of velocity in the (r, θ, z) directions. For a vertical annulus, the following set of equations is valid:

$$\nabla \cdot \mathbf{u} = 0 \tag{1}$$

$$v = 0 \tag{2}$$

$$u = -p_r \tag{3}$$

$$w = -p_z + \frac{Ra}{Pe} T \tag{4}$$

$$\mathbf{u} \cdot \nabla T = \frac{1}{Pe}\left(T_{rr} + \frac{1}{r} T_r + T_{zz}\right). \tag{5}$$

For a horizontal annulus, the governing equations are

$$\nabla \cdot \mathbf{u} = 0 \tag{6}$$

$$u = -p_r - \frac{Ra}{Pe} T \cos\theta \tag{7a}$$

$$v = -\frac{p_\theta}{r} + \frac{Ra}{Pe} T \sin\theta \tag{7b}$$

$$w = -p_z \tag{7c}$$

$$\mathbf{u} \cdot \nabla T = \frac{1}{Pe}\left(T_{rr} + \frac{1}{r} T_r + \frac{1}{r^2} T_{\theta\theta} + T_{zz}\right). \tag{8}$$

In the equations given above, the velocity scale is $\bar{w}$, the mean velocity entering the annulus, and the

NOMENCLATURE

A, c	empirical constants in grid generation
g	acceleration due to gravity
J, Y	Bessel functions of first and second kind
K	permeability
k_f	effective thermal conductivity of porous medium
L	length of annulus
Nu	inner Nusselt number, $1/T_w$
Nu_i	inner Nusselt number at an axial location
Nu_l	local Nusselt number as a function of θ and z
Nu_f	value of Nu_i under forced flow conditions
$\overline{Nu}$	average value of Nu_i over the length of the annulus
$\hat{p}$	component of pressure driving mean flow
$\tilde{p}$	component of pressure driving secondary flow
Pe	Peclet number, $\bar{w}\Delta R/\alpha$
q_w	heat flux on the inner wall
r, θ, z	cylindrical coordinates; θ measured from the gravity vector
R_1, R_2	inner and outer radii
ΔR	characteristic dimension, $R_2 - R_1$
Ra	Rayleigh number, $g\beta\Delta TK\Delta R/\nu\alpha$
T	temperature
T_w	inner wall temperature
ΔT	characteristic temperature, $q_w\Delta R/k_f$
u, v, w	components of velocity
$\bar{w}$	mean flow in axial direction.

Greek symbols

α	thermal diffusivity of saturated porous annulus
β	volumetric expansion coefficient
η	transformed radial coordinate
λ_n	nth eigenvalue
ν	kinematic viscosity
Ψ	secondary-flow stream function.

Other symbol

∇	gradient operator in cylindrical coordinates.

Subscript

r	derivative with respect to r

Superscripts

$'$	derivative with respect to argument
n	current location in the z-direction.

length scale is $R_2 - R_1$, the annular gap width. The two dimensionless parameters which arise in this problem are the Rayleigh number and the Peclet number, which are defined in the Nomenclature. Equations (1)–(8) are solved subject to a constant heat flux on the inner boundary and an isothermally cooled outer boundary. Only one half of the horizontal annulus ($\theta = 0$–π) is considered, due to the symmetry of the problem. The boundary conditions are

$$\begin{aligned} r = R_1, &\quad T_r = -1 \\ r = R_2, &\quad T = 0 \\ \theta = 0, \pi, &\quad T_\theta = 0 \text{ (horizontal)} \\ z = 0, &\quad w = 1, \quad u = v = 0, \quad T = 0 \\ z = L, &\quad T_z = 0 \text{ (vertical).} \end{aligned} \tag{9}$$

METHOD OF SOLUTION

Vertical annulus

Equations (1)–(5) and the associated boundary conditions are solved as a two-dimensional elliptic boundary-value problem. To this end, a stream function Ψ is introduced, which is obtained from $u = (1/r)\Psi_z$ and $w = (1/r)\Psi_r$. The stream-function equation is obtained by eliminating pressure between equations (3) and (4). The equations are solved by a control-volume/finite difference scheme, as described by Gosman *et al.* [8]. The algebraic matrix equation is solved by a Gauss–Seidel method. The convective terms in the energy equation are differenced by the second upwind procedure given by Roache [9]. All results have been obtained on a grid with 81 points in the z-direction and 41 in the r-direction. The nodes in the r-direction are arranged in such a way that the region close to the walls has a finer discretization. The iterations continue until a convergence criterion of 0.01% is met between successive iterations. The choice of the grid is based on the requirement of adequate energy balance for the entire annulus. This value is within 3% for the results given in this work.

Horizontal annulus

Equations (6)–(8), describing flow in a horizontal annulus, are three-dimensional, and a direct solution is expected to be computationally expensive. The following simplifications have been made to convert the three-dimensional problem to a two-dimensional marching problem. This process of parabolizing the flow equations is described by Anderson *et al.* [10], in the context of Navier–Stokes equations. The implications of using this method for Darcian flow are different, and so it is elaborated upon here. It is first assumed that the derivatives in the mean flow (i.e. z) direction are small, so that T_{zz} may be dropped from equation (8). This permits a marching procedure for T, from a

known initial profile for temperature of the incoming flow. The assumption that T_{zz} is much smaller than other diffusion-related derivatives requires that Pe not be small, i.e. $Pe > 1$. The second assumption is with regard to pressure. The pressure field is taken to be of the form

$$p(r, \theta, z) = \hat{p}(z) + \bar{p}(r, \theta). \tag{10}$$

This is justified whenever there is a mean flow which does not undergo reversal and a superimposed secondary flow driven by the pressure field $\bar{p}(r, \theta)$. From equation (6c), it follows that

$$w = -\hat{p}(z). \tag{11}$$

This equation can be solved by using the constraint of mass conservation, i.e.

$$\int_{R_1}^{R_2} \int_0^{\pi} rw(r, \theta, z)\, dr\, d\theta = \frac{\pi}{2}(R_2^2 - R_1^2).$$

Using equation (11), this gives $p(z) = -1$, and so $w(r, \theta, z) = 1$ everywhere. This step decouples equations (7a) and (7b) from equation (7c) and permits the use of a stream function in place of the secondary pressure field $\bar{p}(r, \theta)$. Defining the stream function Ψ from $u = (-1/r)\Psi_\theta$ and $v = \Psi_r$, the three-dimensional continuity equation is now identically satisfied by Ψ. The equation governing Ψ is obtained from equations (7a) and (7b) as

$$\Psi_{rr} + \frac{1}{r}\Psi_r + \frac{1}{r^2}\Psi_{\theta\theta} = \frac{Ra}{Pe}\left(\frac{1}{r}\cos\theta T_\theta + T_r \sin\theta\right). \tag{12}$$

With the velocity field now determined, the energy equation is solved by marching along the z-coordinate.

Solutions of equations (8) and (12) are again obtained by finite differences. The initial temperature of the fluid as it enters the annulus is taken as zero, which is also the outer wall temperature. Equation (8) is cast in the form

$$T_z = \frac{1}{Pe}(\nabla^2 T) - \left(\frac{1}{r}(ruT)_r + \frac{1}{r}(vT)_\theta\right) \equiv S_1$$

and equation (12) as

$$\nabla^2 \Psi - S_2 = 0.$$

Marching in the z-direction is fully implicit, and the velocity–temperature calculation is fully coupled. The iteration scheme is generated from

$$\frac{T^{n+1} - T^n}{\Delta z} = S_1^{n+1} \tag{13a}$$

$$[\nabla^2 \Psi - S_2]^{n+1} = 0. \tag{13b}$$

The node concentration next to the walls is accomplished by a grid generation method [11]. The variable r is replaced by η, where η satisfies

$$\eta_{rr} + \frac{1}{r}\eta_r = -\sum_{i=1}^{2} A \operatorname{sign}(\eta - \eta_i) \exp(-c|\eta - \eta_i|). \tag{14}$$

Values of $A = 10$ and $C = 0.2$ provide sufficient nodal concentration near the walls of the annulus. In equation (14), $\eta_1 = R_1$ and $\eta_2 = R_2$. Details of the use of grid generation in cylindrical geometries may be found in ref. [12]. A 21×21 grid is used in the r- and θ-directions. In the z-direction, the step size is non-uniform, ranging from 0.005 very close to the inlet to 0.04 at large distances from it. This choice of grid ensures an energy balance of within 5%, and good agreement with analytical results, as described later. The energy balance is however poor for values of $z < 0.02$. At the inlet the local Nusselt number goes to infinity, and no attempt has been made to improve the results in this region.

Calculations for the vertical annulus were performed on a VAX 11/780 computer. For the choice of the grid and convergence criterion used in this work, the CPU time was found to be 2 min per run. The CPU time depends strongly on the initial guess, and hence on the change in Rayleigh and Peclet numbers from one run to the next. For a given Peclet number, the change in Ra was kept around 100 in the present study.

Calculations for the horizontal annulus were performed on a DEC-1090 computer. Marching in the z-direction was accomplished using a variable integration step to keep the computing time per step almost uniform. The CPU time per run (up to $z \sim 10$) was found to be 10 min. The thermal development length decreases for higher values of Ra. This behaviour is discussed in the next section. Hence, calculations of strong mixed convection flow were found to require less time in comparison to forced flow.

Analytical solution

Forced flow in a porous annulus can be solved analytically for the temperature field. The mathematical problem is

$$T_z = \frac{1}{Pe}\left(T_{rr} + \frac{1}{r}T_r\right)$$

$$r = R_1, \quad T_r = -1$$

$$r = R_2, \quad T = 0$$

$$z = 0, \quad T = 0. \tag{15}$$

The solution is obtained by separation of variables [13] and is given as

$$T(r, z) = R_1 \ln\frac{R_2}{r} + \sum_{n=1}^{\infty} C_n R(\lambda_n, r) \exp\left(-\lambda_n^2 \frac{z}{Pe}\right) \tag{16}$$

where

$$R = J_0(\lambda_n r) Y_0(\lambda_n R_2) - J_0(\lambda_n R_2) Y_0(\lambda_n r)$$

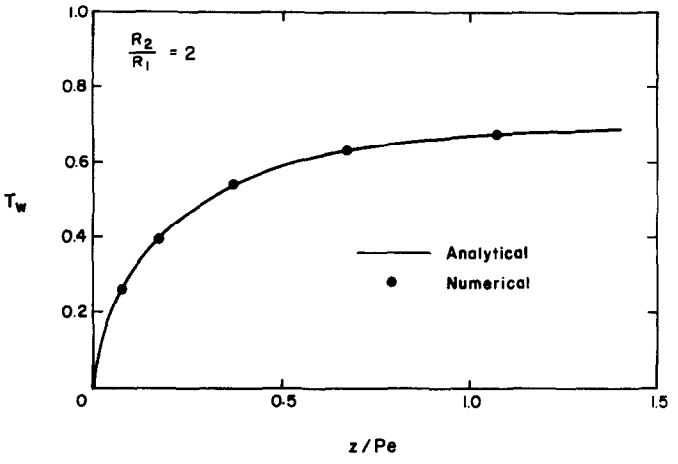

FIG. 1. Comparison of analytical and numerical solutions for inner wall temperature: $Ra = 0$.

$$C_n = -\frac{\int_{R_1}^{R_2} rR_1 \ln\frac{R_2}{r} R(\lambda_n, r)\,dr}{\int_{R_1}^{R_2} rR^2(\lambda_n, r)\,dr}$$

and λ_n is the root of

$$J_0'(\lambda_n R_1) Y_0(\lambda_n R_2) - J_0(\lambda_n R_2) Y_0'(\lambda_n R_1) = 0.$$

Validation of numerical results

The numerical procedures described above for both the horizontal and vertical annuli have been tested against the analytical solution for forced flow conditions. Figure 1 shows a plot of inner wall temperature in the annulus obtained from the two numerical schemes and the analytical solution given by equation (16). The numerical solutions overlap each other, and agreement with the analytical solution is also good. The other extreme of free convection in a horizontal annulus has been compared with the results of Caltagirone [4]. Despite differences in the numerical schemes used and in the number of nodal points, the agreement is within 5% of the average Nusselt number.

RESULTS AND DISCUSSION

The primary intent of this work is to study mixed convective flow and heat transfer from heated cylinders for the range of parameters encountered in the nuclear waste disposal problem. Since the permeability of compacted soil is low, the Rayleigh number range to be expected here is $0 < Ra < 100$. Based on the velocity of ground water movement, the Peclet number range is also limited to $0 < Pe < 10$. In the event of cracking of the soil around the waste disposal unit, higher Peclet numbers may occur. For $Pe > 100$, (and $0 < Ra < 100$), heat transfer is controlled by the superimposed flow, and the analytical solution should be adequate. For $Ra > 500$ (and $0 < Pe < 10$), heat transfer is predominantly due to free convection, and the results available in the literature (e.g. Caltagirone [4], Prasad and Kulacki [2]) should be useful. The limiting case of simultaneously high Peclet number and high Rayleigh number is not considered to be probable. However, the techniques described in this work are also applicable to this problem. It has not been studied here due to its excessive nodal requirement and consequent computational effort. The other limiting case of $Pe \to 0$ (but not equal to zero) and $Ra > 500$ cannot be solved by the marching technique described here for a horizontal annulus. This is because of omission of the term T_{zz} from the energy equation. It must be solved as a fully three-dimensional elliptic problem. All results presented in this paper are for a radius ratio of 2.

Referring to Fig. 1, it can be seen that the wall temperature attains a fully developed value for $z/Pe \approx 1$. This is related to the growth of the thermal boundary layer on the heated wall, and the fully developed state corresponds to a boundary-layer thickness of $(R_2 - R_1)$, the annular gap width. Hence, for $Pe = 10$, the development length for forced flow is about 10. Beyond this value, energy is conducted from the inner to the outer wall, and energy transported by flow is zero. For both the vertical and horizontal annuli, a length of about $z = 10$ has been used in this work for $Pe = 10$ to study the mixed convection problem.

Figure 2 shows a comprehensive plot of local Nusselt number on the inner wall as a function of distance for a vertical annulus. Curves 1 and 2 correspond to free convective motion of the fluid. For $Ra = 1$, fluid motion barely affects heat transfer. However, for $Ra = 100$ (curve 2), boundary layers grow on each wall, and the Nusselt number varies sharply with z. Curves 3 and 4 are for mixed convective flow, with a Peclet number of superimposed flow equal to 10. For $Ra = 1$ (curve 3), the influence of buoyancy is almost absent. It can be seen that the Nusselt number variation for $Ra = 100$ and $Pe = 0$ corresponds closely in magnitude to $Ra = 1$ and $Pe = 10$. It may then be

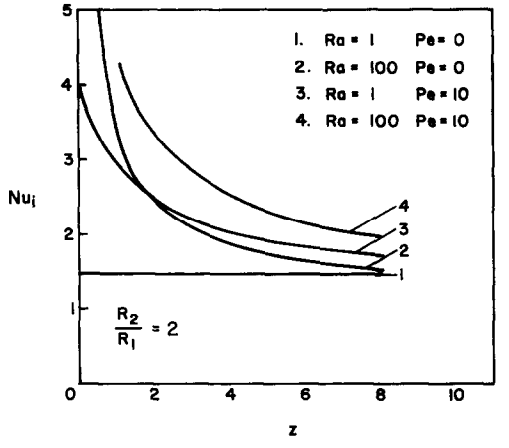

FIG. 2. Inner wall Nusselt number as a function of axial distance for a vertical annulus.

concluded that the velocities generated due to buoyancy at $Ra = 100$ are of a magnitude leading approximately to $Pe = 10$. Hence, at $Ra = 100$, values of Pe much larger than 10 would make forced convection predominant. At $Pe = 10$, values of Ra much larger than 100 would make free convection the primary mechanism of heat transfer. Curve 4 shows the combined effect of free and forced convection on the local Nusselt number.

Figure 3 shows a plot of average inner Nusselt number of the entire vertical annulus of length $L = 10$ as a function of Rayleigh number. The incremental change in Nusselt number as Ra increases is about the same for all three Peclet numbers shown. Hence, the percentage change in the average heat transfer drops at higher Pe. A surprising result is the sharp change in Nu as Peclet number changes from 0 to 1. For $Ra = 100$, the free convective motion generated can be expected to be more vigorous than the flow at $Pe = 1$. However, as one moves from $Pe = 0$ (no prescribed flow) to $Pe > 0$, a fundamental change in flow pattern occurs. At $Pe = 0$ ($Ra > 0$), a recirculation pattern sets in which is completely destroyed for $Pe > 0$. This pattern is replaced by thin thermal boundary layers, which give rise to large heat transfer rates. Hence, the jump in average Nusselt number from $Pe = 0$ to 1 is essentially a phenomenon related to inlet conditions of flow. As the length of the vertical annulus is increased, thus jump can be expected to reduce.

In the configuration considered above, buoyancy aids mean flow and there is an increase in heat transfer rate from the heated wall over the forced convection value. It is also possible to consider external flow in the direction parallel to the gravity vector, against the direction of free convective motion. Results of this calculation are not presented here. This is because the solution is seen to be very sensitive to the exit flow boundary condition. The gradient boundary condition used in this work at $z = L$ assumes that the flow is not seriously disturbed at this location and beyond. This is not realized in the opposed flow arrangement. It is recommended that measured profiles of velocity and temperature be used instead in future calculations.

Figure 4 shows a plot of local inner Nusselt number of a horizontal annulus as a function of the axial coordinate and for various Rayleigh numbers. At $Ra = 0$, the curve for forced flow (equation (16)) is reproduced. As Ra increases, the curve shifts upwards, since heat transfer is due to the combined mechanism of mean flow and the buoyant secondary flow. There is no sudden change in structure of flow as one goes from $Pe = 0$ to $Pe > 0$. This is because the secondary flow is quite small very close to the entrance, where the thermal boundary layers are thin. Its effect increases downstream, and a fully developed state is attained, which depends on the value of Ra. Hence, for $Ra < 500$, forced flow dominates free convection over the range $0 < z < 1$. The extent of mixed convection depends on the magnitude of Ra, and is reduced at large Ra. Buoyancy can be seen to accelerate the growth of the boundary layer, and also determine the heat transfer rate, once this layer fills the annular gap. At $Ra = 100$, the fully developed Nusselt number is 2.298; at $Ra = 500$, it is 3.94. These values are identical to the average Nusselt numbers obtained from two-dimensional analysis of free convection in a horizontal porous annulus. (See, for example, ref. [14].) Figure 5 shows a plot of the extent of secondary flow along the length of the annulus. The effect of this

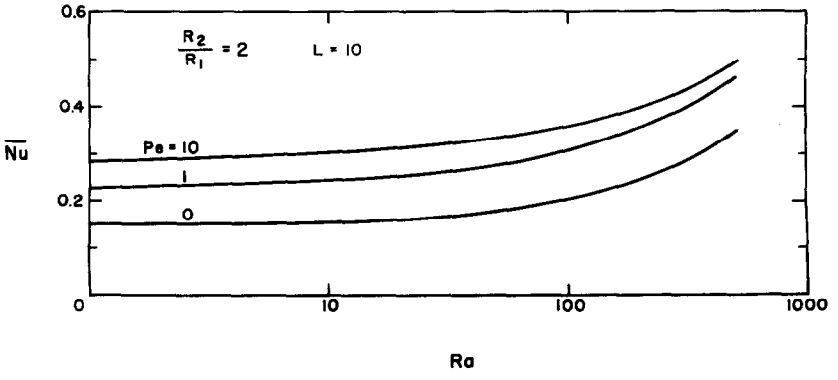

FIG. 3. Average Nusselt number of a vertical annulus as a function of Rayleigh number.

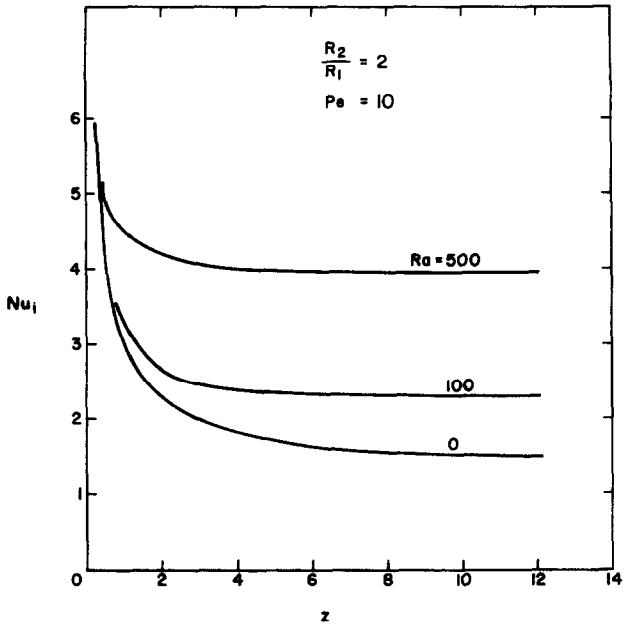

FIG. 4. Inner wall Nusselt number as a function of axial distance for a horizontal annulus.

flow is to give rise to a skewness in Nusselt number variation in the angular direction. In Fig. 5, the Nusselt number has been normalized by its value at the axial location if forced flow conditions had prevailed. At $z = 0.275$, the skewness is small, but it increases with distance. At $z = 10.675$, the full variation in Nu seen in free convection in a horizontal porous annulus is recovered.

Figure 6 shows a sketch of velocity vectors in an annulus with a heated inner wall for $Ra = 0$ and $Ra > 0$, but for finite Peclet numbers. In Fig. 6(a), the changes in the velocity field due to increasing Rayleigh number are shown for a vertical annulus. The enhancement in heat transfer arises from acceleration of flow in the neighbourhood of the heated wall. Figure 6(b) shows changes in velocity for a horizontal annulus. In this problem, heat transfer is governed by the formation of a swirl component of velocity in the annulus.

CONCLUSIONS

The following observations have been made on the basis of the calculations presented in this study. These

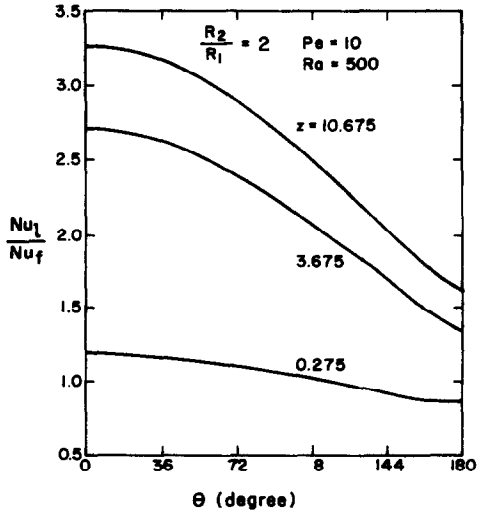

FIG. 5. Local Nusselt number as a function of the angular coordinate in a horizontal annulus.

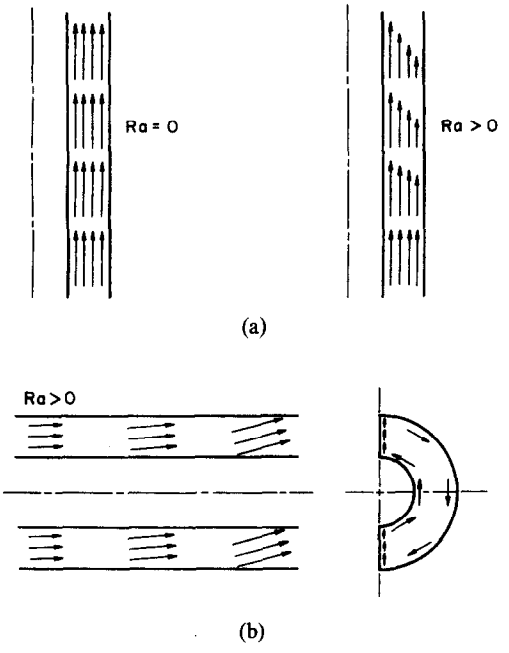

FIG. 6. Sketch of velocity vectors in mixed convection flow in a porous annulus.

are specific to the radius ratio of 2, but no substantial qualitative differences should be expected at other radius ratios. (The development length and Nu–Ra relationship are, however, functions of this radius ratio.)

(1) The forced convection thermal boundary layer grows over a distance of $z \approx Pe$, before it fills the annular gap.

(2) In a vertical annulus, a Peclet number of 10 generates the same order-of-magnitude velocity as $Ra = 100$. Hence, at $Ra = 100$, $Pe > 10$ would give rise to a forced convection regime. Similarly, at $Pe = 10$, $Ra > 100$ would give rise to a free convection regime. For large annulus lengths, the mixed convection Nusselt number approaches the conduction Nusselt number, irrespective of the Rayleigh number. In this conduction regime of fluid movement, buoyant flow is nonzero, but it does not alter the rate of wall heat transfer.

(3) In a horizontal annulus, buoyancy is small very close to the entrance, but increases in the flow direction. At the fully developed state, the Nusselt number is entirely determined by the secondary flow. Hence, the large-distance Nusselt number does not approach the conduction limit, and increases with Rayleigh number. The rate of boundary-layer growth increases with Ra; as a result, the extent of the mixed convection regime diminishes at high Rayleigh numbers.

REFERENCES

1. V. Prasad, Natural convection in porous media—experimental and numerical study for vertical annular and rectangular enclosures. Ph.D. Thesis, University of Delaware (1983).
2. V. Prasad and F. A. Kulacki, Natural convection in a vertical porous annulus, *Int. J. Heat Mass Transfer* **27**, 207–219 (1984).
3. V. Prasad, F. A. Kulacki and M. Keyhani, Natural convection in porous media, *J. Fluid Mech.* **150**, 89–119 (1985).
4. J. Caltagirone, Thermoconvective instabilities in a porous medium bounded by two concentric horizontal cylinders, *J. Fluid Mech.* **76**, 337–362 (1976).
5. Y.-F. Rao, Y. Miki, K. Fukuda, Y. Takata and S. Hasegawa, Flow patterns of natural convection in horizontal cylindrical annuli, *Int. J. Heat Mass Transfer* **28**, 705–714 (1985).
6. P. Ranganathan and R. Viskanta, Mixed convection boundary-layer flow along a vertical surface in a medium, *Numer. Heat Transfer* **7**, 305–317 (1984).
7. J. Bear, *Dynamics of Fluids in Porous Media*. Elsevier, Amsterdam (1972).
8. A. D. Gosman, W. M. Pun, A. K. Runchal, D. B. Spalding and M. Wolfshtein, *Heat and Mass Transfer in Recirculating Flows*. Academic Press, New York (1969).
9. P. J. Roache, *Computational Fluid Dynamics*. Hermosa, Albuquerque, New Mexico (1976).
10. D. A. Anderson, J. C. Tannehill and R. H. Pletcher, *Computational Fluid Mechanics and Heat Transfer*. Hemisphere, Washington, DC (1984).
11. J. F. Thompson (Editor), *Numerical Grid Generation*. Elsevier, Amsterdam (1982).
12. K. Muralidhar and S. I. Guceri, Comparative study of two numerical procedures for free convection problems, *Numer. Heat Transfer* **9**, 631–638 (1986).
13. M. N. Ozisik, *Heat Conduction*. Wiley, New York (1980).
14. K. Muralidhar and F. A. Kulacki, Non-Darcy natural convection in a saturated horizontal porous annulus, *Trans. ASME J. Heat Transfer* **110**, 133–139 (1988).

ECOULEMENT DE CONVECTION MIXTE DANS UN ESPACE ANNULAIRE POREUX SATURE

Résumé—L'écoulement de convection mixte et le transfert thermique sont considérés dans un espace annulaire entre deux cylindres concentriques, rempli d'un matériau poreux saturé de fluide. Le cylindre intérieur est chauffé tandis que le cylindre extérieur est refroidi. On étudie le taux de transfert thermique au cylindre intérieur en fonction de l'écoulement surimposé, avec des effets possibles de flottement. On inclut dans l'étude les espaces annulaires horizontaux et verticaux. Les équations sont résolues numériquement. Les résultats concernent un domaine de nombre de Péclet $0 < Pe < 10$ et de nombre de Rayleigh $0 < Ra < 500$. Le régime de convection mixte est admis être prédominant pour ce domaine des paramètres.

MISCHKONVEKTION IN EINEM GESÄTTIGTEN PORÖSEN RINGRAUM

Zusammenfassung—Die Strömung und der Wärmeübergang bei Mischkonvektion in einem porösen, gesättigten Ringraum zwischen konzentrischen Zylindern werden untersucht. Der innere Zylinder wird beheizt, der äußere gekühlt. Die Wärmeabgabe am inneren Zylinder wird als Funktion der überlagerten Strömung untersucht, wobei mögliche Auftriebseffekte berücksichtigt werden. Sowohl horizontale als auch vertikale Ringräume werden untersucht. Die Strömungsgleichungen werden numerisch gelöst. Die Ergebnisse gelten für Peclet-Zahlen $0 < Pe < 10$ und Rayleigh-Zahlen $0 < Ra < 500$. Es wird erwartet, daß in diesem Parameter-Bereich Mischkonvektion vorliegt.

СМЕШАННОКОНВЕКТИВНОЕ ТЕЧЕНИЕ В НАСЫЩЕННОМ ЖИДКОСТЬЮ ПОРИСТОМ КОЛЬЦЕВОМ СЛОЕ

Аннотация—Рассматривается смешанноконвективное течение и теплоперенос в пространстве между концентрическими цилиндрами, заполненном пористым веществом, насыщенным жидкостью. Внутренний цилиндр нагревается, а внешний охлаждается. С учетом эффектов подъемных сил исследуется интенсивность теплопереноса от внутреннего цилиндра. Изучаются как горизонтальный, так и вертикальный кольцевые зазоры. Численно решаются определяющие уравнения для потока. Получены результаты для чисел Пекле, изменяющихся в диапазоне $0 < Pe < 10$, и диапазона чисел Рэлея $0 < Ra < 500$. Предполагается, что для данного диапазона параметров преобладающим режимом будет смешанная конвекция.